Preparation and properties of clean Si_3N_4 surfaces

V.M. Bermudez[*], F.K. Perkins

Electronics Science and Technology Division, Naval Research Laboratory, Washington, DC 20375-5347, USA

Abstract

In situ chemical methods for preparing atomically-clean surfaces of Si_3N_4 thin films in ultra-high vacuum (UHV) have been studied using X-ray and ultraviolet photoemission, electron energy loss and Auger electron spectroscopies. Prior to the UHV studies, the films (grown ex situ on $Si(1\,0\,0)$ wafers by low-pressure chemical vapor deposition) were characterized using primarily infrared reflection–absorption spectroscopy. A combination of annealing in NH_3 to remove C and deposition of Si (followed by thermal desorption) to remove O is found to be an effective cleaning procedure. Other potential cleaning methods, such as annealing in UHV without in situ chemical treatment and annealing in a flux of H atoms, were also considered and found to be only partly effective. The clean surfaces are disordered but show no evidence of Si–Si bonding (which would indicate N vacancies) in the Si LVV Auger spectrum or in surface-sensitive Si 2p photoemission data. Evidence for surface-related features is seen in the N 1s photoemission and in energy loss spectra in the region of valence excitations; however, no indication of occupied surface states near the valence band maximum is seen in ultraviolet photoemission spectra. Preliminary results for O_2 chemisorption show adsorbate-induced features in the Si_3N_4 band gap and also evidence for changes in surface potential due to adsorption.
© 2004 Elsevier B.V. All rights reserved.

1. Introduction

Silicon nitride (Si_3N_4) is an important material for use in electronic devices. Dense films of this material inhibit diffusion of water, oxygen and Na^+ ions and are widely used as passivation layers in integrated circuits. The wear resistance and chemical inertness of Si_3N_4 also make it useful as a protective coating for magnetic thin films in disk drives. For these applica-

tions, thin films are often grown by chemical vapor deposition (CVD) or by sputter deposition (SD). In contrast to the situation for most other electronic materials, little is known about the preparation of clean and stoichiometric surfaces of Si_3N_4 after growth or about their chemisorption properties. In this work we are concerned with developing an in situ chemical process for obtaining atomically-clean Si_3N_4 surfaces in ultra-high vacuum (UHV). The properties of the resulting clean surfaces will be characterized, and a preliminary evaluation of the effects of exposure to O_2 will be reported. The primary diagnostic tools used here are Auger electron, electron

[*] Corresponding author. Tel.: +1 202 767 6728;
fax: +1 202 767 1165.
E-mail address: bermudez@estd.nrl.navy.mil (V.M. Bermudez).

Report Documentation Page		*Form Approved* *OMB No. 0704-0188*

Public reporting burden for the collection of information is estimated to average 1 hour per response, including the time for reviewing instructions, searching existing data sources, gathering and maintaining the data needed, and completing and reviewing the collection of information. Send comments regarding this burden estimate or any other aspect of this collection of information, including suggestions for reducing this burden, to Washington Headquarters Services, Directorate for Information Operations and Reports, 1215 Jefferson Davis Highway, Suite 1204, Arlington VA 22202-4302. Respondents should be aware that notwithstanding any other provision of law, no person shall be subject to a penalty for failing to comply with a collection of information if it does not display a currently valid OMB control number.

1. REPORT DATE **OCT 2003**	2. REPORT TYPE	3. DATES COVERED **00-00-2003 to 00-00-2003**
4. TITLE AND SUBTITLE **Preparation and properties of clean Si3N4 surfaces**		5a. CONTRACT NUMBER
		5b. GRANT NUMBER
		5c. PROGRAM ELEMENT NUMBER
6. AUTHOR(S)		5d. PROJECT NUMBER
		5e. TASK NUMBER
		5f. WORK UNIT NUMBER
7. PERFORMING ORGANIZATION NAME(S) AND ADDRESS(ES) **Naval Research Laboratory,Electronics Science and Technology Division,4555 Overlook Avenue SW,Washington,DC,20375**		8. PERFORMING ORGANIZATION REPORT NUMBER
9. SPONSORING/MONITORING AGENCY NAME(S) AND ADDRESS(ES)		10. SPONSOR/MONITOR'S ACRONYM(S)
		11. SPONSOR/MONITOR'S REPORT NUMBER(S)

12. DISTRIBUTION/AVAILABILITY STATEMENT
Approved for public release; distribution unlimited

13. SUPPLEMENTARY NOTES

14. ABSTRACT

In situ chemical methods for preparing atomically-clean surfaces of Si3N4 thin films in ultra-high vacuum (UHV) have been studied using X-ray and ultraviolet photoemission, electron energy loss and Auger electron spectroscopies. Prior to the UHV studies, the films (grown ex situ on Si(1 0 0)wafers by low-pressure chemical vapor deposition) were characterized using primarily infrared reflection?absorption spectroscopy. A combination of annealing in NH3 to remove C and deposition of Si (followed by thermal desorption) to remove O is found to be an effective cleaning procedure. Other potential cleaning methods, such as annealing in UHV without in situ chemical treatment and annealing in a flux of H atoms, were also considered and found to be only partly effective. The clean surfaces are disordered but showno evidence of Si?Si bonding (which would indicateNvacancies) in the Si LVVAuger spectrum or in surface-sensitive Si 2p photoemission data. Evidence for surface-related features is seen in the N 1s photoemission and in energy loss spectra in the region of valence excitations; however, no indication of occupied surface states near the valence band maximum is seen in ultraviolet photoemission spectra. Preliminary results for O2 chemisorption show adsorbateinduced features in the Si3N4 band gap and also evidence for changes in surface potential due to adsorption.

15. SUBJECT TERMS

16. SECURITY CLASSIFICATION OF:			17. LIMITATION OF ABSTRACT	18. NUMBER OF PAGES	19a. NAME OF RESPONSIBLE PERSON
a. REPORT **unclassified**	b. ABSTRACT **unclassified**	c. THIS PAGE **unclassified**	**Same as Report (SAR)**	**14**	

Standard Form 298 (Rev. 8-98)
Prescribed by ANSI Std Z39-18

energy loss, ultraviolet photoemission and X-ray photoemission spectroscopies (AES, ELS, UPS and XPS, respectively).

Various Si_3N_4 cleaning processes involving wet-chemical treatment and/or Ar^+-ion bombardment have been evaluated [1–3] using XPS or ion scattering spectroscopy (ISS). The wet-chemical methods considered to date [1,2] do not appear to be completely effective in removing surface contamination. For Si_3N_4 films grown by low-pressure chemical vapor deposition (LPCVD) on Si(1 0 0), cleaning by Ar^+-ion bombardment followed by annealing in UHV was found, using ISS [3], to leave the surface almost free of oxygen and terminated in Si. Si_3N_4 films grown in situ on Si(1 0 0) or (1 1 1) surfaces by exposure to NH_3 at high temperature were also found [4,5] to be terminated in a Si-rich layer. However, recent work [6] using high-resolution XPS for Si(1 1 1) surfaces nitrided with NH_3 has indicated an abruptly-terminated and stoichiometric Si_3N_4 surface. Hence, the surface termination of a clean Si_3N_4 substrate is uncertain at this point and may depend on the methods used for film growth and for surface preparation.

The effect of Ar^+-ion bombardment on SiN_x materials has been studied extensively, and preferential removal of N is a recurring problem. Again, the results may depend quantitatively on the method used for film growth. Films grown by LPCVD [7–10], atmospheric-pressure CVD [10], plasma-enhanced chemical vapor deposition (PECVD) [7,11–13], thermal nitridation of Si [14] or SD [15,16] have been investigated using XPS, AES and other methods. Most studies conclude that some degree of damage (e.g., Si–N bond-breaking) and preferential sputtering is unavoidable, with the effects being more severe at lower ion energies. Films grown by LPCVD appear to be less susceptible to these effects than are those grown by other means [7], possibly due to the much lower H content in LPCVD material. However, there are exceptions in that some studies conclude that preferential sputtering either does not occur or else is independent of ion energy in the 2–4 keV range [10], or that it can be virtually eliminated by appropriate choice of Ar^+-ion energy ($\geq$2 keV) [15,16].

Ions other than Ar^+ have also been considered. H^+ ions in the range of about 0.2–1 keV [17] rapidly sputter LPCVD Si_3N_4 with preferential removal of N. For a sample grown by CVD on Si, He^+ ions [18]

preferentially remove Si (N) for an ion energy of 0.5 (2.0) keV. (Analogous results were also reported for Ar^+ ions.) Although other studies have not observed a preferential removal of Si, these findings imply that stoichiometric sputtering could be achieved with a carefully-chosen He^+- or Ar^+-ion energy. For Si nitride layers formed by N_2^+ ion implantation into Si(1 0 0) [19], N_2^+ ions in the range of 0.25–5.0 keV preferentially removed N. For LPCVD layers, Xe^+ ions in the range of 0.5–3.0 keV were seen [7] to have essentially the same effect as Ar^+ ions.

In addition, some studies report that the damage and the change in Si/N atom ratio caused by ion impact can be reversed by electron bombardment [8,10], by standing in UHV [8,9] or by annealing [17], all of which could result from diffusion of N from the bulk to the surface. However, Chao et al. [12] have cautioned that this apparent ''healing'' effect, which is deduced from changes in the fine-structure of the Si LVV Auger spectrum, could also arise from reaction of the damaged surface with O-containing impurities in the UHV background.

In the present work we seek to develop an in situ chemical method for preparing atomically-clean Si_3N_4 surfaces UHV, one that does not involve ion bombardment. In the future this will permit, by comparison with data for ion-bombarded surfaces, a determination of the extent to which cleaning by sputtering affects surface structure and stoichiometry. It will also provide a method by which Si_3N_4 surfaces can be prepared for subsequent UHV surface-science studies of phenomena such as chemisorption. In situ chemical cleaning is also expected to be useful for preparing surfaces of very thin films, which might be destroyed by ion bombardment, and for cleaning high-surface-area samples such as powders, porous materials and nanowires, which are not readily amenable to standard ion-bombardment methods.

2. Experimental

Thin ($\sim$45 nm) Si_3N_4 films were grown[1] by LPCVD on Si(1 0 0) wafers. The growth temperature of 750 °C, using SiH_2Cl_2 and NH_3 as reagents, is known

---

[20] to result in stoichiometric Si_3N_4. Films grown by this means were characterized using external-reflection infrared reflection–absorption spectroscopy (IRRAS), which gives access to the Si_3N_4 phonon modes. Samples to be used for this purpose were grown by depositing a ∼200 nm thick layer of either $TiSi_2$ or PtSi on the Si(1 0 0) substrate prior to Si_3N_4 growth. The silicide layer serves as a buried metal layer (BML) for IRRAS (see below). For comparison of the IRRAS data, some Si_3N_4 films were also formed by SD. In this case, prior to nitride growth, ∼200 nm of Al was sputter-deposited onto the Si wafer to form the BML. About 2 nm of Co was deposited prior to the Al to enhance adhesion. It is noted that these special BML samples, for which the Si_3N_4 film was also thicker (see below) than for typical samples, were used only in the external-reflection IRRAS experiments. The bulk of the work reported here, including some IR internal-reflection measurements, was performed on thin films grown on bare Si substrates.

Prior to the UHV experiments, the sample was subjected to a wet-chemical cleaning procedure to reduce the level of surface contamination. The sample was immersed for 5 min in a 4:1:1 mixture of deionized (DI) $H_2O:H_2O_2:NH_4OH$ at 80 °C, followed by rinsing under flowing DI H_2O. The sample was then immersed for 3 min in 7:1 buffered oxide etch solution at room temperature and rinsed under flowing DI H_2O. The sample was then mounted in a conventional UHV chamber with a base pressure after bake-out of ∼5×10^{-11} Torr. The sample could be resistively heated and the temperature of the Si substrate measured with an IR pyrometer. For AES, a double-pass cylindrical mirror analyzer (CMA) was used in the first-derivative, ''non-retard'' mode with a 2 eV peak-to-peak modulation amplitude (except where noted) and a 3 keV, ∼6 μA primary beam incident normal to the surface. Surface-sensitive ELS was performed similarly to AES but with a 90 eV, 0.7 μA primary beam and 0.5 eV modulation amplitude, giving a resolution (full-width at half-maximum [FWHM] of the elastic peak) of 0.8 eV.

For UPS and XPS, the CMA was used in the ''retard'' (constant-resolution) mode with pulse-counting detection. The UPS excitation source was the He(II) ($hv = 40.8$ eV) line of a DC discharge in He gas. The CMA pass energy was typically 25 eV, giving a total instrumental resolution of ∼0.40 eV. For XPS,

two different excitation sources were used. The 151.64 eV Mζ line of a Zr anode (with a 2 μm thick Ag foil window) was used for surface-sensitive Si 2p spectra. After numerical processing [21] to reduce the effect of the finite source line width, the total resolution was about 0.75 eV. Other XPS data were obtained using the Mg $K\alpha_{1,2}$ line ($hv = 1253.6$ eV), with a CMA pass energy of 50 or 100 eV, corresponding to a total resolution (quadrature sum of CMA resolution and X-ray line width) of about 1.0 or 1.7 eV, respectively.

For external-reflection IRRAS, polarization modulation (PM) was combined with a Fourier transform spectrometer (see Ref. [22] and works cited) in an external-reflection geometry with a ''wide-band MCT'' ($Hg_xCd_{1-x}Te$) detector. A resolution of 8 cm^{-1} was used and 1000 scans averaged in ∼8 min for each data set. Triangle apodization and two-fold zero-filling were performed on the interferogram before Fourier transformation. The quantity $\Delta R/R \equiv (R_s - R_p)/(R_s + R_p)$ was recorded, where R_s (R_p) is the s- (p-) polarized reflectance of the sample. Due to the presence of the BML and to the high (∼80°) angle of incidence relative to the surface normal, only R_p is strongly affected by thin surface layers [22]. The s-polarized beam then serves as a reference, making PM-IRRAS in effect a double-beam experiment. To obtain the spectrum of the Si_3N_4 film itself, the difference spectrum, $\delta(\Delta R/R)$, was obtained from $\Delta R/R$ recorded for a BML with and without a Si_3N_4 film.

Infrared attenuated total reflection (IRATR) data were obtained for 45 nm thick LPCVD films grown on both sides of a Si internal-reflection element (IRE). The IRE was 1 mm thick and 25 mm long with an internal-reflection angle of 60°, giving a total of 14 reflections. The ATR measurements were performed similarly to the IRRAS experiments described above, except that unpolarized light and a pyroelectric detector were used. The reference sample in this case was a bare Si IRE.

H-atom exposure was done using a hot (∼1750 °C) W filament in H_2 (nominally 99.995% pure), with a filament-to-sample distance of about 1 cm. Exposures are given in Langmuirs (L), where $1 L = 10^{-6}$ Torr s, based on the H_2 pressure measured with an ionization gauge. The cracking efficiency for H_2 on W at 1750 °C is reported [23] to be ∼2.5%. High-purity NH_3 was transferred under vacuum to a stainless-steel sampling

cylinder containing Na metal as a drying agent. Exposures were done using a pinhole doser [24] for which the output flux had been calibrated. O_2 (nominally 99.99% pure) was admitted through a leak valve and the pressure measured with a cold-cathode ionization gauge in order to avoid electronic excitation of the molecule. All gases were checked for purity using a quadrupole mass spectrometer mounted in the UHV chamber.

3. Results and discussion

3.1. Characterization of Si_3N_4 films

Due to the complexity of the Si_3N_4 growth process and to the variability of material characteristics noted above and in the literature, it is necessary to investigate the bulk properties of the present samples before undertaking the surface studies.

Fig. 1 shows external-reflection PM-IRRAS data (recorded in a dry N_2 ambient) for typical SD and LPCVD films. These data provide access to the Si_3N_4 phonon modes, which are valuable in assessing film quality. The apparent rise in absorption below ~700 cm^{-1} is due to the decreasing transmission of the ZnSe optical element of the polarization modulator. Fig. 1 also shows numerical simulations obtained using the matrix formulation [25][2] for the polarized reflectance of a multilayer material, together with IR optical constants [26] for Si_3N_4 grown on Si(1 0 0) by PECVD. To the best of our knowledge, these are the most extensive such IR data available for Si_3N_4. The simulation allows comparison of the SD, LPCVD and PECVD results on an equal basis. In Fig. 1a, tabulated [27] IR optical constants were used for the Al BML. In Fig. 1b the TiSi$_2$ BML, for which IR data [28] are available only above ~1000 cm^{-1}, was modeled as metallic W which has similar IR properties [27]. The calculation is qualitatively independent of the exact nature of the BML. The model assumes isotropic and homogeneous materials with ideal interfaces.
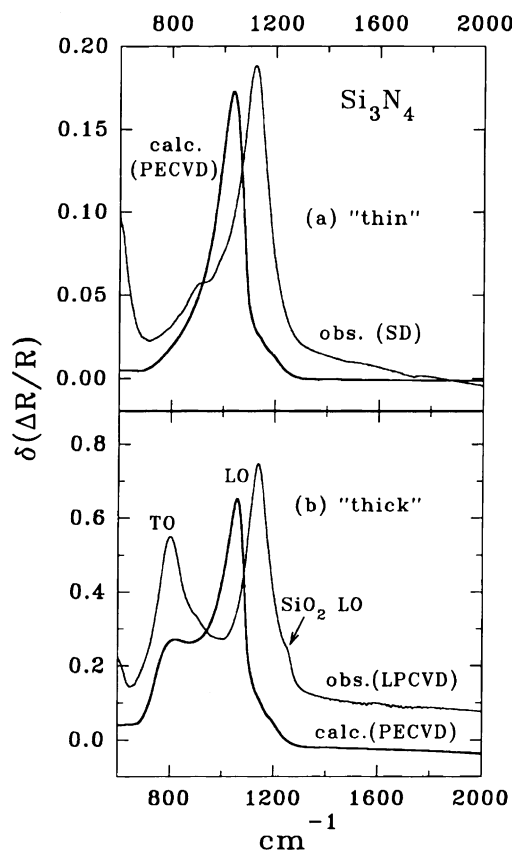
Fig. 1. PM-IRRAS data ("obs.") for: (a) thin SD and (b) thick LPCVD Si_3N_4 films. The calculations ("calc.") employ optical constants [26] for PECVD Si_3N_4. Note the different vertical scales for the two panels. The model film thicknesses of: (a) 60 nm and (b) 500 nm have been arbitrarily adjusted to bring the calculated intensities into approximate agreement with experiment.

The dominant feature in the experimental spectra is the Si_3N_4 longitudinal-optic (LO) phonon at ~1130 cm^{-1}, and data for the thick film also show a transverse-optic (TO) mode at 804 cm^{-1}. Transmission spectra of PECVD Si_3N_4 films show TO modes [26] at 805 and 936 cm^{-1} corresponding to Si–N stretching vibrations for N bonded to three and to two Si atoms, respectively. The presence of both species in PECVD Si_3N_4 is responsible for the broadening seen in the TO region of the simulation, Fig. 1b. H-free LPCVD films [29] show only an 811 cm^{-1} TO mode in this region, in agreement with the present results. For LPCVD films containing H [30], a TO mode asymmetrically broadened to higher energy is seen at about 835 cm^{-1}. Thus, the present LPCVD

films, with a relatively low bulk-H content, show N(–Si–)$_3$ as the dominant species. The LPCVD film (Fig. 1b) also shows a shoulder at ∼1250 cm^{-1} due to SiO$_2$ at the film surface and at the Si$_3$N$_4$/BML interface, as found in XPS sputter-profiling (see below).

Fig. 1 shows the LO mode lying ∼85 cm^{-1} higher for both SD and LPCVD Si$_3$N$_4$ than for PECVD material. It is known [31] that the N/Si ratio in PECVD Si$_3$N$_4$ can deviate substantially from 1.33 and that this leads to a reduction [32] in the LO frequency from the "ideal" value [32,33] of ∼1124–1130 cm^{-1}. Structural inhomogeneity [34] or the presence of H [35] could also cause a red shift of the LO mode in PECVD Si$_3$N$_4$. Previous work [5] has reported high-resolution electron energy loss data for the vibrational spectra of Si$_3$N$_4$ films grown on Si(1 1 1) surfaces by reaction with NH$_3$ at elevated temperature. Modes were found at 480, 710 and 970 cm^{-1}, none of which correspond well to LO or TO modes in either PECVD or LPCVD Si$_3$N$_4$ which suggests that surfaces of films grown by nitriding a Si(1 1 1) surface may be fundamentally different from those of bulk Si$_3$N$_4$.

Fig. 2 shows ATR data (recorded in a dry N$_2$ ambient) which are useful for observing weak absorptions due to trace amounts of H remaining from LPCVD growth. As a result of the long path length through the absorbing Si IRE, the region below ∼1200 cm^{-1} is inaccessible, and the Si$_3$N$_4$ phonons (Fig. 1) are not detectable here. The Si–H and N–H stretching modes occur at 2200 and 3335 cm^{-1}, respectively. The high Si–H frequency is consistent with a stoichiometric Si$_3$N$_4$ film [36] in which (–N–)$_3$Si–H is the dominant silane species. However, a simple interpretation is complicated by the fact that the mode frequency for (–N–)$_3$Si–H in an oxygen-free film is reported [26,36] to be 2170 cm^{-1}, significantly lower than the present value of 2200 cm^{-1}. This could indicate that the Si–H bonds are associated with a small level of O impurity (in the form of a species such as (–N–)$_2$(–O–)Si–H) where the higher electronegativity of O versus N would give rise to a higher Si–H frequency [36]. Alternatively, the H could be bound at Si sites at the Si$_3$N$_4$ surface or at the buried interface with the Si IRE, where higher concentrations of O are expected. The N–H frequency, on the other hand, is characteristic of NH in oxygen-free Si$_3$N$_4$ [26]. Adding O to the film shifts this mode to higher values [26], and –NH$_2$ in Si$_3$N$_4$ would exhibit a stretching mode at

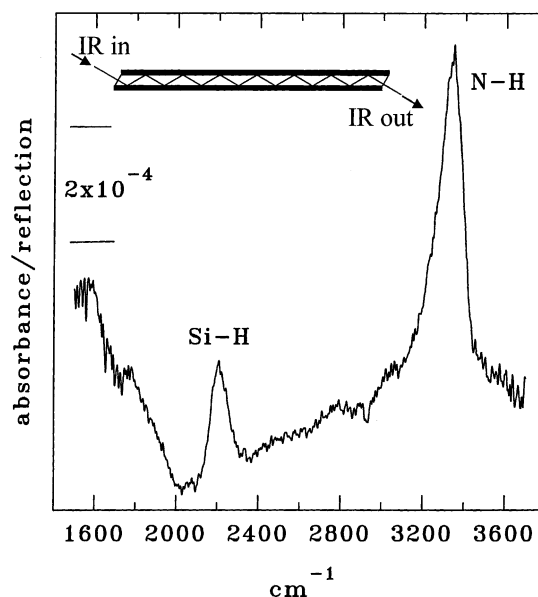
Fig. 2. Unpolarized IRATR data in the Si–H and N–H stretching regions for 45 nm thick LPCVD Si$_3$N$_4$ films grown on both faces of a Si IRE. The inset shows a schematic of the light path through the IRE, with the aspect ratio of the IRE shown to scale and the thickness of the Si$_3$N$_4$ films (filled-in bands) greatly exaggerated.

∼3460 cm^{-1} [37]. It should be noted that the surface cleaning process described below involves annealing in UHV at 1100 °C and that most of the Si–H and N–H groups are expected [38] to decompose at or below this temperature.

The as-received LPCVD films were also characterized using XPS sputter-profiling and ellipsometry. The former results (not shown) indicate a thin surface layer of impurity O and C. For some samples, a thin oxide layer was found at the interface between the Si$_3$N$_4$ film and the substrate. Ellipsometric measurements were done at $\lambda = 632.8$ nm to determine the index of refraction of the Si$_3$N$_4$ which is a useful indicator of material quality. A value of $n = 1.93$ was obtained which is in reasonable agreement with the result ($n = 2.02$) for H-free pyrolytic Si$_3$N$_4$ (see Ref. [39] and works cited). The slightly lower value obtained here could indicate a correspondingly small reduction in the density of the LPCVD film versus a pyrolytic sample.

3.2. Surface cleaning

The first approach was simply to anneal the sample in UHV for periods of 3 or 5 min at temperatures as

high as 1100 °C. Bulk Si_3N_4 is known [40] to be stable at temperatures well in excess of 1000 °C. However, CVD films can exhibit thermally-induced changes at lower temperatures [41–44], due either to loss of H (in the case of PECVD material) or to reaction with the substrate.

After insertion of a new sample, the UHV chamber was first baked at ~150 °C after which the sample was held at 700 °C for several hours until the sample, sample holder, etc. were outgassed and the pressure decreased to $<5 \times 10^{-10}$ Torr. Auger data (Fig. 3a) indicated C and O as the only detectable impurities. A previous study [2] of Si_3N_4 found little or no effect on the level of C and O contamination for a 350 °C anneal in UHV. In the present work, annealing at 1100 °C caused some reduction in the impurity concentration, possibly via desorption of SiO or diffusion into the bulk, but it was not possible to eliminate fully the C and O AES signatures.
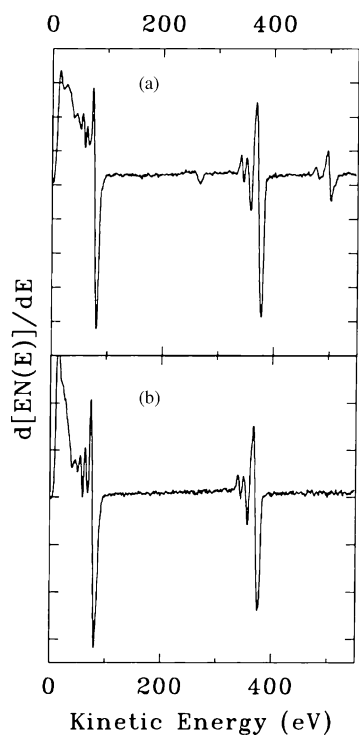

Fig. 3. AES data for: (a) an as-inserted sample after baking the UHV chamber and outgassing the sample and (b) after cleaning. Relative intensities are approximately quantitative. Both spectra have been subjected to a fifth-order, nine-point polynomial smoothing.

Exposure to H atoms is known (e.g., Ref. [45] and works cited) to be useful in cleaning the surfaces of III–V semiconductors without requiring the high-temperature anneal that follows cleaning by ion bombardment. The H atoms are generated either by cracking H_2 on a hot W filament or by a plasma source. Similar results have been reported for Si (see Refs. [46,47] and works cited). For the column-III nitrides, H-atom cleaning was found to eliminate carbon contamination [48] but to be less effective in removing oxides [48,49]. Attention must also be given to the possibility of etching reactions (as have been reported [50] for Si_3N_4 exposed to an H plasma) which could alter the surface stoichiometry.

In the present work, Si_3N_4 films were exposed to H atoms at sample temperatures as high as 950 °C and H_2 exposures as high as ~10^5 L (i.e., ~10^{-4} Torr for 10^3 s). It was found via AES (not shown) that such treatment may cause some reduction in C coverage but that it has little or no effect on the O coverage. It is possible that the higher flux provided by an H plasma source might be more effective in surface cleaning.

Exposure to a flux of NH_3 (~3.5×10^{14} NH_3/cm^2 s for 5 min at a sample temperature of 950 °C) was found to be effective in reducing the C coverage to below the AES detection limit. However, there was little or no effect on the O coverage. This parallels results [48,51] for GaN(0 0 0 1) surfaces which were explained [51] in terms of the different heats of reaction of NH_3 with C (to form $CH_4 + N_2$) and with O (to form $H_2O + N_2$). (It has recently been shown [52] that, at a sufficiently high NH_3 pressures, it is possible to remove both C and O from GaN(0 0 0 1) surfaces.) Having removed the C impurity it now remains to eliminate the O.

"Si flux cleaning" or "Si flux annealing" was described by Kaplan [53] as a method for preparing atomically-clean SiC surfaces. Here, either SiC is annealed in the presence of a nearby resistively-heated Si wafer or else Si is vapor-deposited in situ onto the room-temperature SiC substrate which is subsequently annealed in UHV to desorb excess Si. It is thought that, during annealing, impurity O desorbs as SiO [54] and impurity C reacts to form epitaxial SiC. It has also been shown [48,55] that SiH_4 can be used in place of a hot Si wafer as a source of Si. Use of a gaseous Si source should facilitate the "conformal" cleaning of porous or high-surface-area substrates. It is further

noted that the presence of a Si surface layer has been reported [40] to impede the thermal decomposition of a Si_3N_4 substrate.

Oxygen was easily removed by first depositing Si while maintaining the Si_3N_4 at ~950 °C. The Si wafer, facing the sample at a distance of about 1 cm, was resistively heated to ~1070 °C for about 3 min. Following this, AES data (not shown) indicated a strong free-Si LVV peak at 91 eV super-imposed on the corresponding Si_3N_4 feature at 81 eV (see below). The excess free-Si was desorbed by annealing in UHV at 1100 °C for about 5 min, giving the Auger spectrum shown in Fig. 3b. The C and O signals are below the AES detection limits. Based on standard peak-to-peak height (PPH) sensitivity factors and the noise level in the data, these limits correspond to atomic fractions of about 2 and l%, respectively, for a model in which impurities are uniformly distributed throughout the AES sampling depth.

The parameters given here for the NH_3 and Si treatments (e.g., total NH_3 dose, annealing times and temperatures, etc.) are only indicative, and the effect of varying these quantities has not been studied in detail.

3.3. Characterization of the clean surface

Fig. 4 shows in detail the Si LVV and N KLL Auger line shapes for a clean Si_3N_4 surface which agree well with results for a stoichiometric SD film [56]. The Si LVV spectrum shows no evidence of the narrow free-Si peak at about 90 eV which is characteristic [8,9,12] of damaged or N-deficient Si_3N_4 with Si–Si bonds. The Si LVV spectrum showed no changes in shape over the course of repeated scans of the same area of the surface. Such an effect would indicate damage (e.g., desorption of N or Si–N bond-breaking) by the primary electron beam. Bulk charging of the insulating Si_3N_4 film was negligible since the Si LVV spectrum exhibited no significant shift in energy when the Auger primary beam was varied in the 2–5 keV range. No low-energy electron diffraction pattern was seen, not even a (1×1) pattern from the bulk of the film, which indicates that the Si_3N_4 LPCVD films are disordered. Since no ion bombardment was done, this disorder appears to be intrinsic to the present films and not the result of damage incurred during surface cleaning.
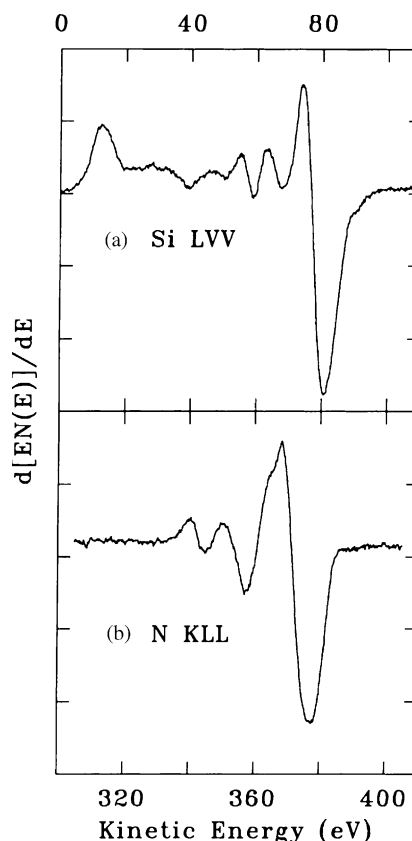

Fig. 4. Si LVV and N KLL Auger spectra (1 eV peak-to-peak modulation) for a clean Si_3N_4 surface. Relative intensities are not quantitative (see Fig. 3). Note the different energy ranges for the two plots.

Fig. 5 shows the Zr Mζ-excited Si 2p XPS, together with the results of a least-squares fit. The Si 2p spin–orbit doublet was represented by a pair of Gaussian-broadened Lorentzians (i.e., Voigt functions[3]) with a splitting of 0.610 eV and a branching ratio of 0.54. Both parameters were fixed at values found [57] for elemental Si and are not expected to be significantly material-dependent. Although the 2p Lorentzian width in elemental Si [57] is very small ($\leq$35 meV), a better fit (as judged by the residual spectrum) was obtained with a finite Lorentzian broadening included in the model line shape. The energy, intensity and widths (both Gaussian, Γ_G, and Lorentzian, Γ_L) were all

---

[3] The Voigt line shape was obtained accurately, by numerical convolution of the appropriate Gaussian and Lorentzian functions, rather than in approximate form.
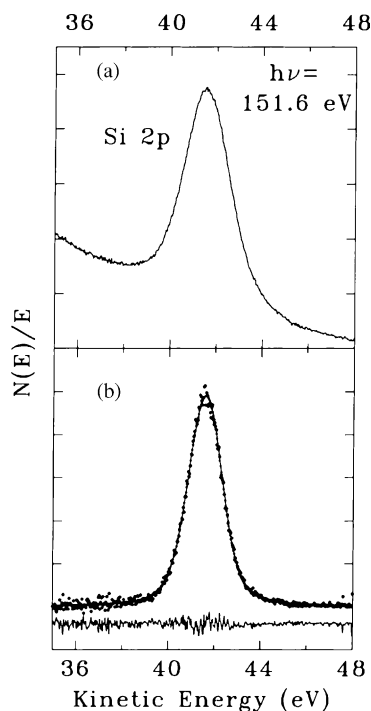
Fig. 5. Zr Mζ-excited Si 2p XPS data for a clean Si_3N_4 surface: (a) shows the raw data. In (b), the points show the spectrum after numerical processing [21] to reduce instrumental broadening. The solid curve shows the result of least-squares fitting with the sum of a Gaussian-broadened Lorentzian spin–orbit doublet and a third-order polynomial background. For display, the background obtained in the fit has been subtracted. Also shown is the residual spectrum (fit minus data) which cannot be statistically weighted because the numerical processing removes intensity from the raw data. The spectra in panel (b) have been displaced vertically for clarity.

adjustable in the fitting process, as were the coefficients of a cubic polynomial included to represent the small background not removed by the data reduction [21]. There is no indication of satellite structure, such as a feature due to Si–Si bonding which would appear at lower binding (higher kinetic) energy (e.g., Ref. [16]). The lack of Si–Si bonding is consistent with the Si LVV spectrum discussed above. These results argue against the presence of a surface layer resembling elemental Si, as was seen [4] in surface-sensitive XPS for Si_3N_4 grown in situ on Si(1 0 0) by reaction with NH_3.

A further experiment was done by depositing Si in situ on the clean Si_3N_4 surface and recording the Mg $K\alpha_{1,2}$-excited Si 2p spectrum (not shown). The Si thickness was ~2–3 Å, based on the attenuation of

the PPH of the substrate N KLL signal in AES, assuming a uniform coverage. The thickness estimate used an effective electron attenuation length (EAL) in Si of $\lambda_e = 10.7$ Å at the N KLL energy which was obtained from a standard semi-empirical database [58]. The energy difference between the substrate and overlayer XPS peaks was 2.7 eV, which corresponds well with the difference (2.74 eV [6]) between 2p binding energies for elemental Si and for the Si^{4+} formal oxidation state (FOS) in Si_3N_4. In contrast, the Si^{3+} FOS would exhibit a 2p energy shift of about 2.2 eV relative to elemental Si [6]. The Si 2p XPS results as a whole then indicate that only one Si FOS is detectable, up to and including the surface, and that this is the Si^{4+} state.

The Mg $K\alpha_{1,2}$-excited N 1s XPS peak (Fig. 6) could not be fitted well with only a single line. An additional component at lower kinetic energy (KE) was required, the neglect of which resulted in structure above the noise level in the residual spectrum and in an increase
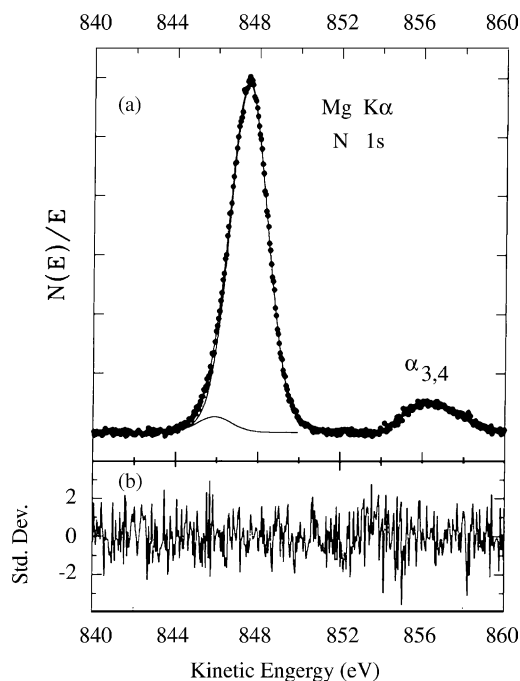

Fig. 6. Mg Kα-excited N 1s XPS data at a total resolution of about 1 eV: (a) shows the raw data (points) and the fitted components (lines). The polynomial background function obtained in the fit has been subtracted for display. "$\alpha_{3,4}$" labels the feature due to a satellite in the Mg Kα source spectrum. (b) shows the spectrum of statistically-weighted residuals, which gives $\chi^2 = 1.14$.

in χ^2 (to ~1.4–1.6). The fit places this feature ~1.7 eV below the main peak with a relative area of about 4%. The fit shown in Fig. 6 took into account the fine-structure of the Mg K$\alpha_{1,2}$ doublet [59], which is replicated in the N 1s peak shape. Lorentzian broadening of the main peak was allowed in order to account for the finite Lorentzian width [59] of the source line. For all three components (i.e., the main peak, the weak satellite and the K$\alpha_{3,4}$ feature), the Gaussian FWHMs were similar (1.6–2.1 eV) for different fits and data sets. This increases confidence in the results since spurious fits often return very different Gaussian widths for various components of the same XPS peak.

The presence of this weak feature was entirely reproducible for repeated surface preparations and XPS measurements. On the other hand, the N 1s spectrum (not shown) for a clean surface with a ~6–7 Å thick layer of Si deposited in situ showed no indication of such a feature. In this case, a fit of comparable quality ($\chi^2 = 1.19$) was obtained with only the main component (and the $\alpha_{3,4}$ feature). Annealing in UHV to desorb the Si led to a return of the satellite. It is unknown whether the effect of the adsorbed Si is to decrease the intensity of the satellite or to shift it to higher KE such that it can no longer be separated from the main peak. Furthermore, fitting the Mg K$\alpha_{1,2}$-excited Si 2s and 2p lines (not shown) did not reveal any form of satellite. These results indicate that the slight asymmetry in the N 1s peak, which necessitates including the satellite in the fit, is not an artifact arising from, e.g., an asymmetric CMA transmission function or an inhomogeneous surface potential. The effect of depositing Si further suggests that this feature is surface-related. The data were also checked for the absence of an effect due to re-adsorption of NH$_3$ from the UHV background (a remnant of the surface preparation) by briefly annealing the sample at 900 °C to desorb any NH$_3$, after the chamber pressure had dropped below 5×10^{-10} Torr, and recording a spectrum.

Inelastic scattering and shake-up processes can be ruled out as the source of the satellite since ELS data (see below) reveal no significant loss features below about 4 eV. Previously a shake-up feature was reported [60] to lie 12 eV below the main N 1s peak for Si(1 0 0) surfaces exposed to NO and nitrided with NH$_3$. This was assigned to a $\pi \rightarrow \pi^*$ excitation at a planar Si(–N–)$_3$ site. In a high-resolution, surface-sensitive XPS study [6] of Si(1 1 1) surfaces nitrided with NH$_3$, a satellite was observed at 0.66 eV lower KE than the main N 1s peak and tentatively assigned to N–N bonds at the surface. The present resolution and surface sensitivity are not such that this particular feature would be detectable. Previous results [61] for an LPCVD sample, after heating to 1200 °C in N$_2$, showed a satellite at 4.6 eV lower KE than the main N 1s line which was also assigned to N–N bonds.

The fraction of the total signal originating from surface atoms can be estimated as ~$d_s/(\lambda_e \cos \varphi)$, where $\lambda_e = 19.9$ Å is the N 1s photoelectron effective EAL [58] in Si$_3$N$_4$, and $\varphi = 42°$ is the CMA collection angle. The "thickness" of the surface layer is estimated as $d_s \approx 1$ Å, approximately half the Si–N bond length. This gives ~6.8% for the surface contribution which is in reasonable agreement with the ~4% relative area of the satellite peak. No conclusive assignment of this feature is possible at this time; although, it appears possible that a surface species involving bonds between N atoms may be important.

Fig. 7 shows surface-sensitive ELS data. The peak energies correspond to inflection points in the first-derivative spectrum and were determined more precisely by numerically differentiating to obtain
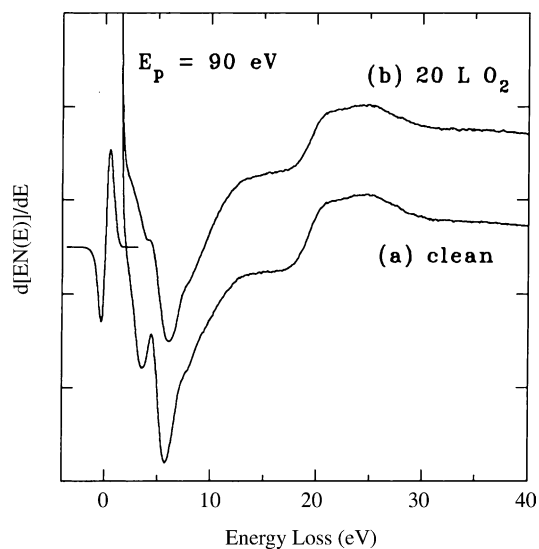

Fig. 7. Surface-sensitive ELS data for: (a) a clean surface and (b) after a 20 L O$_2$ exposure. The elastic peak is shown, reduced in amplitude by a factor of ~400, at the zero of the energy loss. The spectra have been displaced vertically for clarity.

second-derivative spectra (not shown). For the clean surface, the peak energies are in reasonable agreement with previous results [62] for an ion-bombarded LPCVD sample. Major loss peaks are seen in Fig. 7 at 4.1, 6.6 and 19.3 eV (versus 4.6, 6.8 and 18.6 eV in Ref. [62]), and additional small features are found in the ~8–13 eV range in the second-derivative spectra, in agreement with Ref. [62]. The band gap reported [63–65] for H-free Si_3N_4 lies in the range of 5.1–5.4 eV; hence, only the 4.1 eV loss falls below this energy.

The 19.3 eV loss is due to volume plasmon excitation, as shown by the appearance of loss satellites close to this energy (21.5 eV) in core-level XPS (see below). It may be significant that the plasmon appears at lower energy under more surface-sensitive conditions (Fig. 7) than when excited by the higher-energy (~1 keV) photoelectrons. A reduction in the Si_3N_4 plasmon frequency has previously [66] been ascribed to the presence of excess Si; however, as noted above, it is unlikely that the surfaces studied here involve such species. In particular, exposure to O_2, which would be expected to chemisorb at excess-Si sites, had little or no effect on the plasmon energy for exposures as large as 500 L. However, the plasmon results do suggest some form of chemical or structural difference between the bulk of the film and the near-surface region.

The origin of the 4.1 and 6.6 eV losses is uncertain. Lieske and Hezel [62] assigned these to "broken Si–N" bonds resulting from ion bombardment and found that they could be removed by annealing. In contrast, the features seen here were not eliminated by 5 min anneals in UHV at 1100 °C. To help determine if these losses are surface related, the sample was exposed to O_2. The main effect of a small exposure is the appearance of additional loss intensity below ~4 eV and a possible attenuation or shift in energy of the 4.1 and 6.6 eV loss features. A tentative conclusion is that the 4.1 and 6.6 eV losses might be surface-related but are not associated with a highly reactive site such as a singly-occupied Si dangling orbital. A possible assignment may be to an orbital involving a bond between surface atoms. The ELS data also suggest that the clean surface chemisorbs O_2, in agreement with the ISS results of Jo et al. [3].

Fig. 8 shows He(II)-excited UPS data for the valence band (VB) before and after exposure to O_2, together with the theoretical density of states (DOS)
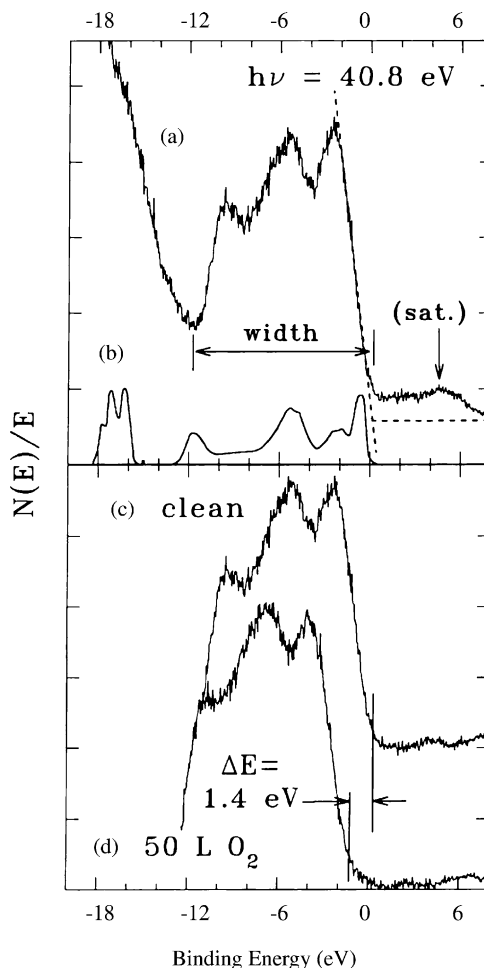

Fig. 8. He(II)-excited UPS data for the valence band of Si_3N_4. Trace (a) shows raw data for the clean surface, and (b) shows the theoretical DOS of Roberston [67]. Binding energy is referenced to the VBM, and the vertical scales are arbitrary. The spectra have been displaced vertically for clarity. The straight lines in (a) illustrate the method used to locate the VBM by linear extrapolation of the edge to zero intensity. The horizontal arrow shows the estimated total width of the VB. The feature labeled "sat.", and the emission between it and the VBM, is due largely to excitation by the 48.4 eV satellite of the main He(II) line at 40.8 eV. Traces (c) and (d) show the results of applying the procedure for reducing the satellite contribution (see text). Trace (c) is for the clean surface (same data as in (a)), and (d) is the result of a 50 L O_2 exposure. Binding energies are referenced to the VBM of (c). The O_2-induced rigid shift of the VB is indicated at the VBM, located as in trace (a).

given by Roberston [67]. With the present excitation source, only the upper-VB is accessible. The deeper-lying states, ~17 eV below the valence band maximum (VBM), are overlapped by the edge of the

upper-VB spectrum excited by the intense He(I) line ($hv = 21.2$ eV) and by the secondary-electron tail of the He(II)-excited upper-VB. The overall shape of the spectrum differs from He(II) UPS data for samples that were either not atomically clean [64] or else were subjected to ion bombardment [68]. However, the three-peaked structure and the ~12 eV total width of the VB are in agreement with these results and with theory [67].

The method used in Fig. 8 to locate the bulk VBM presumes the absence of significant surface-state emission in this region, which would cause an *apparent* shift of the VBM to a higher KE, relative to that of the bulk. In order to make effects near the VBM easier to discern, a procedure was applied to reduce the contribution of overlapping VB spectra (sometimes termed "ghosts") which are excited by higher-energy satellites in the He(II) emission spectrum. The corrected intensity takes the form $I_{corr}(E) \approx I_{obs}(E) - \sum_k [\alpha_k I_{obs}(E - \Delta E_k)]$, where α_k is the fraction of the total He(II) intensity in the kth satellite which lies ΔE_k higher in energy than the 40.8 eV line. In the present case, the correction included only the first satellite, which lies at 48.4 eV with an intensity about 20% of that of the main line [69].

Exposing the clean sample to O_2 caused a rigid shift of the whole spectrum by ~1.4 eV to lower KE, which was also seen in the He(I)-excited spectrum (not shown). However, there is no significant change in shape or width of the upper-VB. This suggests that, if surface states are present near the VBM, they do not involve highly-reactive sites such as Si dangling bonds. A further observation is that the upper-VB width (Fig. 8a) is essentially the same as that seen in bulk-sensitive XPS data [68] obtained with Al Kα excitation ($hv = 1486.6$ eV). This argues against a significant surface-state contribution above the VBM in the surface-sensitive He(II) data, the existence of which would cause the VB width to appear to be greater in UPS than in XPS. The present results differ from those of Kim and Yeom [6] for a Si(1 1 1)-(7 × 7) surface nitrided by reaction with NH$_3$ at high temperature. In that case, intense surface-state emission (which was sensitive to adsorbates) was seen at 1.1 eV above the VBM. This is a further indication of the fundamental difference between Si$_3$N$_4$ surfaces of the type studied here and those prepared by in situ thermal nitridation of Si.

A similar O_2-induced rigid shift was seen for a smaller (20 L) O_2 exposure, and briefly annealing the sample at 900 °C reversed the shift shown in Fig. 8c and d. It was also noted, during the Si deposition experiments described above in connection with Si 2p and N 1s XPS, that a thin (~2 Å) Si layer caused a shift of the substrate core levels by about 1 eV to higher KE relative to the clean surface. This was a rigid shift without a significant change in shape or width. Additional shifts suggesting surface charging, relative to the bulk of the film, were observed during XPS and UPS data collection for the clean Si$_3$N$_4$ surface. The X-ray source flux, which is several orders of magnitude greater than that of the He discharge [70], caused the N 1s peak to shift by 1 to 2 eV to lower KE within the first ~2 min of irradiation. In UPS, a rigid shift of the VB by ~1.6 eV to lower KE occurred gradually during prolonged (~75 min) irradiation.

The effects of adsorbates (e.g., O_2 and Si) on the surface potential could arise from a number of factors. These include changes in the secondary-electron emission coefficient, the surface recombination rate of electron–hole (e–h) pairs [70] and the density or population of surface charge traps [71]. Furthermore, the X-ray and UV photo-induced shifts could also be related to the rates of production, ionization and recombination of e–h pairs or to the filling and emptying of charge traps. A more thorough investigation of surface charge traps, energy shifts in photoemission and the effects of adsorbates is beyond the scope of the present work.

The near-surface stoichiometry was estimated using the relative areas of the N 1s and Si 2s peaks (Fig. 9). The Si 2s, rather than the Si 2p, was used in order to avoid complications resulting from the dependence of photoemission intensity on the angle between the X-ray beam and the photoelectron path [72]. This angle is not well defined in the present experimental configuration. However, all photoelectrons from s-states have the same dependence on this angle; hence, the asymmetry factor cancels when computing relative peak areas. For a model in which Si and N are homogeneously distributed throughout the XPS sampling depth, the atomic concentration ratio is given by $C_N/C_{Si} = (I_{N1s}/I_{Si2s})(S_{Si2s}/S_{N1s})$, where I_x is the integrated peak intensity and S_x the sensitivity factor. For S_x we used the empirical results of Wagner et al.
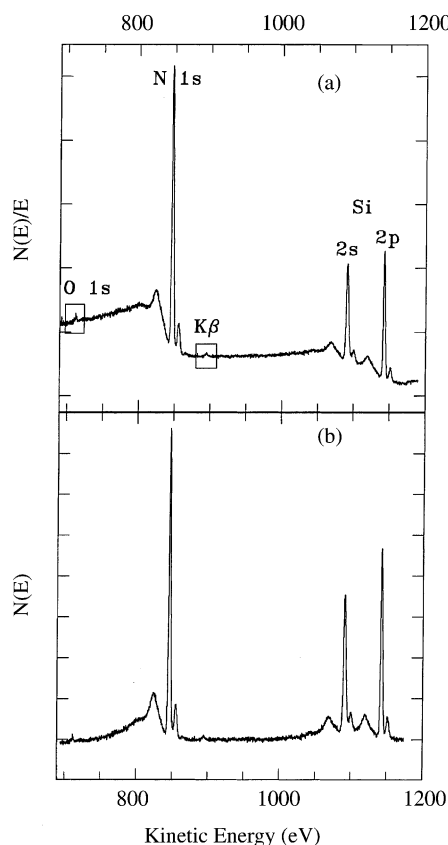
Fig. 9. XPS data for the N 1s–Si 2p region ($\sim$1.7 eV total resolution): (a) shows the raw data, and (b) shows the result of applying the Tougaard procedure for removing the background due to inelastically-scattered electrons. A two-parameter scattering function was used with $B = 2704\,\text{eV}^2$ and $C = 1634\,\text{eV}^2$ (see Refs. [74,75]). The data in (b) have also been corrected for the $1/E$ dependence of the CMA étendue (see text) in constant-resolution mode. The feature marked "Kβ" is due to excitation of the N 1s by the Kβ satellite of the Mg K$\alpha_{1,2}$ line. The weak O 1s signal is due to contamination during the course of data collection. No C 1s feature is detectable near 965 eV.

[73], obtained for a CMA similar to that used here, which gave $(S_{\text{Si 2s}}/S_{\text{N 1s}}) = 0.56$ for Mg Kα excitation.

Fig. 9 shows the data before and after application of the Tougaard [74,75] procedure for removing the background due to inelastically-scattered electrons, which is necessary for an accurate determination of peak areas. As part of this procedure, the spectrum in Fig. 9b has been corrected for the 1/E dependence of the CMA étendue (the product of the CMA transmission and the surface area sampled) on photoelectron KE [72,73]. The peak areas were obtained by least-

squares fitting (as described above) the N 1s and Si 2s regions with a sum of Voigt functions and a low-order polynomial background function in order to separate the main peaks from the K$\alpha_{3,4}$ and plasmon satellites. For the main N 1s and Si 2s peaks, the fits used Γ_{L} values fixed at those obtained in fits to higher-resolution data for these lines. From the resulting $I_{\text{N 1s}}/I_{\text{Si 2s}}$ ratio an estimate of $C_{\text{N}}/C_{\text{Si}} = 1.21 \pm 0.04$ (average of five runs on two samples) was found,[4] which is reasonably close to the ideal value of 1.33 given the uncertainty in the sensitivity factors [73].

4. Conclusions

The surfaces of thin films of LPCVD Si_3N_4 on Si(1 0 0) have been studied, as a function of various in situ chemical cleaning treatments, using primarily AES, ELS, UPS and XPS. The results are as follows.

(1) After outgassing the sample in UHV, a combination of annealing in a flux of NH_3 to remove C and deposition and desorption of Si to remove O is found to be effective in preparing atomically-clean surfaces. Simple high-temperature annealing of the untreated surface in UHV or exposure to H atoms (under the flux conditions attainable here) were found not to be completely effective in eliminating C and O.
(2) The clean surfaces are disordered (as is the bulk of the film); however, there is no indication (in either AES or XPS) of Si–Si bonding associated with N vacancies. The Si is in the +4 formal oxidation state, i.e., four-fold coordinated to N.
(3) Evidence is found for surface-related features in N 1s XPS and in ELS data for valence excitation. It is unknown at present whether these are intrinsic or extrinsic (i.e., defect) states. However, no indication of occupied surface states at or above the VBM is seen in UPS.
(4) The clean Si_3N_4 surface chemisorbs O_2, as shown by effects in surface-sensitive ELS data.

---

[4] The empirical S_x factors in Ref. [73] already include the effect of the $1/E$ dependence of CMA étendue. This was taken into account when quantify the data in Fig. 9b, i.e., the data were not "double-corrected" for the CMA étendue. The uncertainty in $C_{\text{N}}/C_{\text{Si}}$ reflects the scatter in $I_{\text{N 1s}}/I_{\text{Si 2s}}$ and does not include any systematic error in $S_{\text{Si 2s}}/S_{\text{N 1s}}$.

(5) Evidence is seen, in the form of KE shifts in UPS and XPS data, for changes in surface potential due to energetic photon irradiation, to exposure to O_2 and to deposition of Si.

It is anticipated that these results, which should be applicable to other forms of Si_3N_4 such as single crystals, will facilitate detailed studies of well-characterized Si_3N_4 surfaces. Such work has been difficult to perform, to date, due to lack of a suitable method for surface preparation. One important issue, which has not been addressed here, is the question of whether the surface is terminated in Si, in N or in both. Studies employing, e.g., ISS or the vibrational spectroscopy of chemisorbed H atoms should be helpful in this regard. Such information would be essential in the interpretation of data for chemisorption on these surfaces.

Acknowledgements

Note added in proof

Since the submission of this paper, several relevant references have either appeared in print or come to the authors' attention. Egdell et al. [76] have studied differences between the valence plasmon spectra of cubic- and β-Si_3N_4. Several groups [77–80] have studied charge traps in Si_3N_4, and Terekhov et al. [81] have observed a filling of charge traps in the Si_3N_4 gap during 3 keV electron beam irradiation. Bender and Chen [82] have studied the damage and recovery of Si_3N_4 during electron- and ion-beam irradiation.

References

[1] C.A. Desmond, J.J. Olup, P. Abolghasem, J. Folta, G. Jernigan, Electrochem. Soc. Proc. 97 (36) (1998) 171.

[2] S.I. Raider, R. Flitsch, J.A. Aboaf, W.A. Pliskin, J. Electrochem. Soc. 123 (1976) 560.

[3] Y.-S. Jo, J.A. Schultz, S. Tachi, S. Contarini, J.W. Rabalais, J. Appl. Phys. 60 (1986) 2564.

[4] C.H.F. Peden, J.W. Rogers Jr., N.D. Shinn, K.B. Kidd, K.L. Tsang, Phys. Rev. B 47 (1993) 15622.

[5] M.L. Colaianni, P.J. Chen, N. Nagashima, J.T. Yates Jr., J. Appl. Phys. 73 (1993) 4927.

[6] J.W. Kim, H.W. Yeom, Phys. Rev. B 67 (2003) 035304.

[7] F. Pavlyák, I. Bertóti, M. Mohai, I. Biczó, J. Giber, Surf. Interf. Anal. 20 (1993) 221.

[8] E.C. Paloura, S. Logothetidis, S. Boultadakis, S. Ves, Appl. Phys. Lett. 59 (1991) 280.

[9] T. Jung, W. Titel, Phys. Stat. Sol. A 98 (1986) 63.

[10] F. Fransen, R. Vanden Berghe, R. Vlaeminck, M. Hinoul, J. Remmerie, H.E. Maes, Surf. Interf. Anal. 7 (1985) 79.

[11] J.N. Chiang, D.W. Hess, J. Appl. Phys. 65 (1989) 3430.

[12] S.S. Chao, J.E. Tyler, D.V. Tsu, G. Lucovsky, M.J. Mantini, J. Vac. Sci. Technol. A 5 (1987) 1283.

[13] S. Thomas, R.J. Mattox, J. Electrochem. Soc. 124 (1977) 1942.

[14] L. Kubler, R. Haug, E.K. Hill, D. Bolmont, G. Gewinner, J. Vac. Sci. Technol. A 4 (1986) 2323.

[15] G.M. Ingo, N. Zacchetti, High Temp. Sci. 28 (1990) 137.

[16] G.M. Ingo, N. Zacchetti, D. della Sala, C. Coluzza, J. Vac. Sci. Technol. A 7 (1989) 3048.

[17] P.C. Zalm, L.J. Beckers, J. Vac. Sci. Technol. B 2 (1984) 84.

[18] R.S. Bhattacharya, P.H. Holloway, Appl. Phys. Lett. 38 (1981) 545.

[19] C. Palacio, A. Arranz, J. Phys. Chem. B 106 (2002) 4261.

[20] K. Tanaka, A. Tsuge, M. Takiyama, R. Shimizu, Surf. Interf. Anal. 27 (1999) 638.

[21] V.M. Bermudez, J. Electron. Spectrosc. Relat. Phenom. 73 (1995) 249.

[22] V.M. Bermudez, J. Vac. Sci. Technol. A 16 (1998) 2572.

[23] A. Sutoh, Y. Okada, S. Ohta, M. Kawabe, Jpn. J. Appl. Phys. 34 (1995) L1379.

[24] C.T. Campbell, S.M. Valone, J. Vac. Sci. Technol. A 3 (1985) 408.

[25] R.M.A. Azzam, N.M. Bashara, Ellipsometry and Polarized Light, North-Holland, Amsterdam, 1977, Chapter 4.

[26] M. Klanjsek Gunde, M. Macek, Phys. Stat. Sol. A 183 (2001) 439.

[27] E.D. Palik (Ed.), Handbook of Optical Constants of Solids, vol. 1, Academic Press, Orlando, FL, 1985.

[28] A. Borghesi, A. Piaggi, G. Guizzetti, F. Lévy, M. Tanaka, H. Fukutani, Phys. Rev. B 40 (1989) 1611.

[29] G. Beshkov, S. Lei, V. Lazarova, N. Nedev, S.S. Georgiev, Vacuum 69 (2003) 301.

[30] R. Henda, L. Laanab, E. Scheid, R. Fourmeaux, Jpn. J. Appl. Phys. 34 (1995) L437.

[31] D.M. Knotter, T.J.J. Denteneer, J. Electrochem. Soc. 148 (2001) F43.

[32] L. Huang, K.W. Hipps, J.T. Dickinson, U. Mazur, X.D. Wang, Thin Solid Films 299 (1997) 104.

[33] M. Weidner, A. Röseler, Phys. Stat. Sol. A 130 (1992) 115.

[34] K.T. Queeney, M.K. Weldon, J.P. Chang, Y.J. Chabal, A.B. Gurevich, J. Sapjeta, R.L. Opila, J. Appl. Phys. 87 (2000) 1322.

[35] T. Li, J. Kanicki, Appl. Phys. Lett. 73 (1998) 3866.

[36] G.N. Parsons, G. Lucovsky, Phys. Rev. B 41 (1990) 1664.

[37] B.F. Hanyaloglu, E.S. Aydil, J. Vac. Sci. Technol. A 16 (1998) 2794.

[38] S. Narikawa, Y. Kojima, S. Ehara, Jpn. J. Appl. Phys. 24 (1985) L861.

[39] A.B. Djurišić, E.H. Li, Appl. Opt. 37 (1998) 5291.

[40] H.D. Batha, E.D. Whitney, J. Am. Ceram. Soc. 56 (1973) 365.

[41] B. Claflin, G. Lucovsky, J. Vac. Sci. Technol. B 16 (1998) 2154.

[42] C. Boehme, G. Lucovsky, J. Appl. Phys. 88 (2000) 6055.

[43] J. Hong, W.M.M. Kessels, W.J. Soppe, A.W. Weeber, W.M. Arnoldbik, M.C.M. van de Sanden, J. Vac. Sci. Technol. B 21 (2003) 2123.

[44] J.C. Bruyère, B. Reynes, C. Savall, C. Roth, Thin Solid Films 221 (1992) 65.

[45] G.R. Bell, N.S. Kaijaks, R.J. Dixon, C.F. McConville, Surf. Sci. 401 (1998) 125.

[46] R. Kroon, Jpn. J. Appl. Phys. 36 (1997) 5068.

[47] A. Crossley, C.J. Scofield, S. Sugden, R. Clampitt, C. Bradley, Vacuum 46 (1995) 667.

[48] S.W. King, J.P. Barnak, M.D. Bremser, K.M. Tracy, C. Ronning, R.F. Davis, R.J. Nemanich, J. Appl. Phys. 84 (1998) 5248.

[49] T. Ohashi, Y. Saito, T. Maruyama, Y. Nanishi, J. Cryst. Growth 237–239 (2002) 1022.

[50] Y. Kuo, Appl. Phys. Lett. 63 (1993) 144.

[51] V.M. Bermudez, D.D. Koleske, A.E. Wickenden, Appl. Surf. Sci. 126 (1998) 69.

[52] K.M. Tracy, W.J. Mecouch, R.F. Davis, R.J. Nemanich, J. Appl. Phys. 94 (2003) 3163.

[53] R. Kaplan, Surf. Sci. 215 (1989) 111.

[54] H. Hirayama, T. Tatsumi, J. Appl. Phys. 66 (1989) 629.

[55] S.W. King, R.S. Kern, M.C. Benjamin, J.P. Barnak, R.J. Nemanich, R.F. Davis, J. Electrochem. Soc. 146 (1999) 3448.

[56] D. Bouchier, A. Bosseboeuf, Thin Solid Films 139 (1986) 95.

[57] K. Hricovini, R. Günther, P. Thiry, A. Taleb-Ibrahimi, G. Indlekofer, J.E. Bonnet, P. Dumas, Y. Petroff, X. Blase, X. Zhu, S.G. Louie, Y.J. Chabal, P.A. Thiry, Phys. Rev. Lett. 70 (1993) 1992.

[58] C.J. Powell, A. Jablonski, NIST Electron Effective-Attenuation-Length Database, Version 1.0, National Institute of Standards and Technology, Gaithersburg, MD, 2001. Surf. Interf. Anal. 33 (2002) 211. See http://www.nist.gov/srd/nist82.htm for information on obtaining this database.

[59] C. Klauber, Surf. Interf. Anal. 20 (1993) 703.

[60] C. Bater, M. Sanders, J.H. Craig Jr., K.H. Pannell, P.W. Wang, Appl. Surf. Sci. 161 (2000) 328.

[61] V.A. Gritsenko, Yu.N. Morokov, Yu.N. Novikov, Appl. Surf. Sci. 113–114 (1997) 417.

[62] N. Lieske, R. Hezel, Thin Solid Films 61 (1979) 217.

[63] J. Bauer, Phys. Stat. Sol. A 39 (1977) 411.

[64] V.A. Gritsenko, A.V. Shaposhnikov, W.M. Kwok, H. Wong, G.M. Jidomirov, Thin Solid Films 437 (2003) 135.

[65] N. Pic, A. Glachant, S. Nitsche, J.Y. Hoarau, D. Goguenheim, D. Vuillaume, A. Sibai, C. Chaneliere, Solid-State Electron. 45 (2001) 1265.

[66] V.A. Gritsenko, I.P. Petrenko, S.N. Svitasheva, H. Wong, Appl. Phys. Lett. 72 (1998) 462.

[67] J. Roberston, J. Appl. Phys. 54 (1983) 4490.

[68] R. Kärcher, L. Ley, R.L. Johnson, Phys. Rev. B 30 (1984) 1896.

[69] J. Reader, C.H. Corliss, W.L. Wiese, G.A. Martin, Wavelengths and Transition Probabilities for Atoms and Atomic Ions, NSRDS-NBS 68 National Bureau of Standards Gaithersburg, MD, 2001, 1980.

[70] J.P. Long, V.M. Bermudez, Phys. Rev. B 66 (2002) 121308.

[71] K. Hirose, K. Sakano, K. Takahashi, T. Hattori, Surf. Sci. 507–510 (2002) 906.

[72] D. Briggs, M.P. Seah (Eds.), Practical Surface Analysis, Wiley, Chichester, UK, 1983.

[73] C.D. Wagner, L.E. Davis, M.V. Zeller, J.A. Taylor, R.H. Raymond, L.H. Gale, Surf. Interf. Anal. 3 (1981) 211.

[74] S. Tougaard, C. Jansson, Surf. Interf. Anal. 20 (1993) 1013.

[75] S. Tougaard, Surf. Interf. Anal. 25 (1997) 137.

[76] R.G. Egdell, V.E. Henrich, R. Bowdler, T. Sekine, J. Appl. Phys. 94 (2003) 6611.

[77] H. Guo, W. Maus-Friedrichs, V. Kempter, J. Shi, Nucl. Instr. Meth. Phys. Res. B 173 (2001) 463.

[78] Y. Aya, A. Ando, S. Yamasaki, K. Wakisaka, Jpn. J. Appl. Phys. 42 (2003) L1321.

[79] M. Naich, G. Rosenman, Ya. Roizin, M. Molotskii, Solid-State Electron. 48 (2004) 477.

[80] H. Takeuchi, T.-J. King, J. Electrochem. Soc. 151 (2004) H44.

[81] V.A. Terekhov, V.N. Seleznev, É.P. Domashevskaya, Fiz. Tekh. Poluprovodn. 28 (1994) 636;
V.A. Terekhov, V.N. Seleznev, É.P. Domashevskaya, English transl.: Semiconductors 28 (1994) 381.

[82] H. Bender, W.D. Chen, Surf. Interf. Anal. 15 (1990) 38.